electronics

MDPI

Article

Effective Receiver Design for MIMO Visible Light Communication with Quadrichromatic LEDs

Manh Le Tran † and Sunghwan Kim *,†

School of Electrical Engineering, University of Ulsan, Ulsan 44610, Korea; manh288@gmail.com

* Correspondence: sungkim@ulsan.ac.kr

† These authors contributed equally to this work.

Received: 31 October 2019; Accepted: 20 November 2019; Published: 21 November 2019

Abstract: In this paper, we propose a receiver designing principle for the multiple-input multiple-output (MIMO) visible light communication (VLC) systems with quadrichromatic light emitting diodes (QLEDs). To simultaneously transmit multiple data streams, the system consists of multiple QLEDs and multiple receivers; each includes four photodiodes (PDs). We optimize the Euclidean distance of the received signal over some constraints by considering the normal vectors of the receivers. The numerical results show that our proposed receiver design has a better bit error rate (BER) performance in comparison with the conventional receiver.

Keywords: visible light communications; quadrichromatic light emitting diodes; multi-color crosstalk; receiver design

1. Introduction

Visible light communication (VLC) with many attractive features has recently gained much attention because of the increasing demand for seamless mobile data connectivity [1,2]. To further improve the transmission rate of VLC systems, multiple input and multiple output (MIMO) has also been widely investigated and demonstrated to be a highly effective technique that can be employed in VLC systems [3].

Meanwhile, light emitting diodes (LEDs) and photo detectors (PDs) are utilized as transmitters and receivers in general VLC systems, respectively. Multi-color red/green/blue (RGB) LED with better color rendering index and multi-channel parallel transmission can provide a higher transmission rate with a lower error rate in comparison with ordinary LED [4]. Moreover, to improve the color qualities of white illumination light; quadrichromatic LED (QLED), usually with red/amber/green/blue (RAGB) colors, has been suggested as an alternative to RGB LED [5]. Color shift keying (CSK) is a modulation method that exploits the diversity of a multi color LED to modulate the data with the intensity signals of different colors [6]. The authors in [7] recently proposed an enhanced CSK with QLED and considered various illumination qualities.

Moreover, the general communication through VLC channels mainly depends on the availability of line-of-sight (LOS) link. Various studies [8,9] have shown that the orientation and the mobility of the receiver are the two most important factors affecting the quality of the LOS link in VLC. The hemispheric receiver (HR) is one of the most representative angle diversity receivers (ADR) [10] to achieve highly uncorrelated MIMO-VLC channels through altering the orientation angles of the PDs. Since the HR has a fixed value of the PDs orientation, it can not guarantee a good performance in all scenarios of receiver locations.

In this paper, we focus on designing the receivers of the MIMO-VLC systems that are composed of QLEDs. The optimization problem of maximizing the minimum Euclidean distance (ED) of the received signal that considers the normal vectors of the receivers under constraints is solved with the help of

the Taylor expansion method. Moreover, a two-stage iterative algorithm is proposed to determine the optimal orientation with various initial input solutions. The simulation results demonstrate that the proposed method provides a better bit error rate (BER) performance in comparison with the conventional one, where the fixed orientation of the receiver is employed.

Notation: Throughout this paper, $\mathbf{I}_x$ and $\mathbf{1}_{x\times y}$ denote an $x \times x$ identity matrix and an $x \times y$ matrix with all elements as one, respectively. Furthermore, $(.)^T$ denotes transpose, $\|.\|$ stands for the Frobenius norm. $\otimes$ and $\circ$ denote the Kronecker product and the element-wise product, respectively. The operator vec $(\mathbf{X})$ is a column vector resulting from stacking all the columns of $\mathbf{X}$.

2. System Model

In this paper, a MIMO-VLC system with N_t QLEDs and N_r receivers (each receiver has four PDs and RAGB filters) are utilized to transmit data information as a $4N_t \times 4N_r$ MIMO system shown with modulation order M in Figure 1. The transmitted symbol $\mathbf{x}_m$ is a vector of size $4N_t \times 1$, where $\mathbf{x}_m \in \mathcal{S}, m = 1, 2, ..., M$. The constellation $\mathcal{S} = \{\mathbf{x}_1, ..., \mathbf{x}_M\}$ where M is the order of modulation with the transmission rate is $R = \log_2 M$ bps. Moreover, vector $\mathbf{x}_m$ can be expressed as $\mathbf{x}_m = \left[\mathbf{x}_{m,\mathrm{R}}^T, \mathbf{x}_{m,\mathrm{A}}^T, \mathbf{x}_{m,\mathrm{G}}^T, \mathbf{x}_{m,\mathrm{B}}^T\right]^T$ that denotes the mean current of the corresponding red, amber, green, and blue LED chips of all N_t RAGB-LEDs for the m-th sending symbol. Moreover, the modulated signal vector of size $N_t \times 1$ corresponding to each color is $\mathbf{x}_{m,c} = \left[x_{m,c}^1, x_{m,c}^2, ..., x_{m,c}^{N_t}\right]^T$, where c denotes the LED color, $c \in \{\mathrm{R,A,G,B}\}$. In this paper, each QLED is assumed to employ the general CSK constellation that satisfies the maximum total power [7]. The nonnegative signals also need to satisfy the maximum amplitude value constraint to avoid the clipping distortion and the chromaticity constraint [5]. Moreover, since the design of the transmit signal is not our focus, some issues such as the nonlinear, flickering, or synchronization effect are assumed to be perfect [5–7,10].

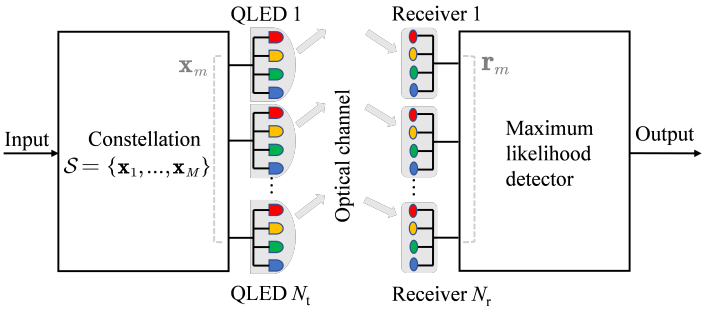

Figure 1. System model.

Meanwhile, a data stream is mapped to a symbol vector chosen from the above constellation $\mathcal{S}$. After transmitting through an optical channel, the received signal vector can be given by

$$\mathbf{r}_m = \mathbf{H}\mathbf{x}_m + \mathbf{n}, \tag{1}$$

where $\mathbf{n}$ is the noise vector with shot noise and thermal noise. The noise is assumed as the zero-mean additive white Gaussian (AWGN) noise with a covariance matrix $\sigma^2\mathbf{I}_{4N_r}$ [3]. $\mathbf{H}$ denotes the channel matrix between the transmitters and the receivers with optical filters. We consider herein the crosstalk between adjacent colors and the $4N_t \times 4N_r$ mutli-color channel matrix $\mathbf{H}$ in [5] can be expressed by two matrices as

$$\begin{aligned}\mathbf{H} &= \begin{bmatrix} (1-\epsilon)\,\mathbf{H}^{\mathrm{R}} & \epsilon\mathbf{H}^{\mathrm{A}} & \mathbf{0} & \mathbf{0} \\ \epsilon\mathbf{H}^{\mathrm{R}} & (1-2\epsilon)\,\mathbf{H}^{\mathrm{A}} & \epsilon\mathbf{H}^{\mathrm{G}} & \mathbf{0} \\ \mathbf{0} & \epsilon\mathbf{H}^{\mathrm{A}} & (1-2\epsilon)\,\mathbf{H}^{\mathrm{G}} & \epsilon\mathbf{H}^{\mathrm{B}} \\ \mathbf{0} & \mathbf{0} & \epsilon\mathbf{H}^{\mathrm{G}} & (1-\epsilon)\,\mathbf{H}^{\mathrm{B}} \end{bmatrix} \\ &= \hat{\mathbf{H}} \circ \mathbf{W},\end{aligned} \tag{2}$$

with $4N_t \times 4N_r$ size matrices $\mathbf{W} = \begin{bmatrix} \mathbf{1-\epsilon} & \boldsymbol{\epsilon} & \mathbf{0} & \mathbf{0} \\ \boldsymbol{\epsilon} & \mathbf{1-2\epsilon} & \boldsymbol{\epsilon} & \mathbf{0} \\ \mathbf{0} & \boldsymbol{\epsilon} & \mathbf{1-2\epsilon} & \boldsymbol{\epsilon} \\ \mathbf{0} & \mathbf{0} & \boldsymbol{\epsilon} & \mathbf{1-\epsilon} \end{bmatrix}$, $\hat{\mathbf{H}} = \begin{bmatrix} \mathbf{H}^{\mathrm{R}} & \mathbf{H}^{\mathrm{A}} & \mathbf{H}^{\mathrm{G}} & \mathbf{H}^{\mathrm{B}} \\ \mathbf{H}^{\mathrm{R}} & \mathbf{H}^{\mathrm{A}} & \mathbf{H}^{\mathrm{G}} & \mathbf{H}^{\mathrm{B}} \\ \mathbf{H}^{\mathrm{R}} & \mathbf{H}^{\mathrm{A}} & \mathbf{H}^{\mathrm{G}} & \mathbf{H}^{\mathrm{B}} \\ \mathbf{H}^{\mathrm{R}} & \mathbf{H}^{\mathrm{A}} & \mathbf{H}^{\mathrm{G}} & \mathbf{H}^{\mathrm{B}} \end{bmatrix}$, where $\epsilon \in [0, 0.5)$ denotes the crosstalk interference ratio. Furthermore, the $N_t \times N_r$ submatrix $\mathbf{H}^c$ denotes the channel coefficients between the N_t QLEDs and N_r receivers, which can be written as

$$\mathbf{H}^c = \begin{bmatrix} h^c_{11} & \cdots & h^c_{1N_t} \\ \vdots & \ddots & \vdots \\ h^c_{N_r1} & \cdots & h^c_{N_rN_t} \end{bmatrix},$$

where h^c_{ij} represents the gain factor between the j-th QLED's chip of the c color and the i-th receiver's PD of c color. For simplicity, since both QLEDs and multi-color receivers are assumed to be assembled in a compact package, and the distances between the transmitters and the multi-color receivers are much larger than either the physical size of the QLED clusters or the receiver clusters; hence, both could be viewed as points [5] and [7], respectively. Consequently, we can consider the same channel matrices $\mathbf{H}^c$ for $c \in \{\mathrm{R,A,G,B}\}$ and omit the color notation c for a simple representation.

Furthermore, the LOS link mainly contributes to the received power at the receiver side; therefore, as an initial exploration, we only consider the room with very low reflection coefficients. In other words, the received signal can be considered to contain only the LOS link for simplicity [8]. Consequently, we have the following channel coefficient between each LED from the j-th QLED and each PD from the i-th receiver [1]

$$h_{ij} = \begin{cases} \frac{(\gamma+1)A_r\delta}{2\pi d^2_{ij}} \cos^{\gamma}\left(\phi_{ij}\right) \cos\left(\theta_{ij}\right), & 0 < \theta_{ij} \leq \theta_{\mathrm{fov}}, \\ 0, & \theta_{ij} > \theta_{\mathrm{fov}}, \end{cases} \tag{3}$$

where ϕ_{ij} is the angle of emergence with respect to the transmitter axis and θ_{ij} is the angle of incidence with respect to their normal axes, respectively. A_r, θ_{fov}, and δ denote the effective area of the detector, the field-of-view (FOV) semiangle of the detector, and the responsivity of the receiver, respectively. d_{ji} is the distance between the j-th QLED and the i-th receiver. The Lambertian mode order γ is $\gamma = \frac{-\ln 2}{\ln(\cos \Phi_{1/2})}$, where $\Phi_{1/2}$ is the half power semiangle of the QLED. Moreover, at the receiver side, assuming perfect knowledge of the channel and ideal time synchronization, the maximum likelihood (ML) detector [7] can be employed. More specifically, by minimizing the Euclidean distance between the received signal vector $\mathbf{r}$ and all possible received signals $\mathbf{Hx}$ as $\tilde{\mathbf{x}} = \arg\min_{\mathbf{r}} \|\mathbf{r} - \mathbf{Hx}\|^2$, the receiver tries to decide which symbol $\tilde{\mathbf{x}}$ was transmitted.

3. Proposed Receiver Design

3.1. Problem Formulation

Denote $\mathbf{t}_j$, $\mathbf{u}_i$, and $\mathbf{v}_{ji}$ as the normal vector of the j-th QLED, the normal vector of the i-th receiver, and the vector between positions of the j-th QLED and the i-th receiver as in Figure 2. Without loss of generality, we normalize the normal vector lengths to 1, that is, $\|\mathbf{t}_j\| = 1$, $\|\mathbf{u}_i\| = 1$. Consequently, we have $\cos\phi_{ij} = \frac{\mathbf{t}^T_j\mathbf{v}_{ji}}{\|\mathbf{v}_{ji}\|}$, $\cos\theta_{ij} = \frac{-\mathbf{v}^T_{ji}\mathbf{u}_i}{\|\mathbf{v}_{ji}\|}$. Therefore, as described in [10], in the condition of $0 < \theta_{ij} \leqslant \theta_{\mathrm{fov}}$, the channel coefficient in (3) can be rewritten as

$$h_{ij} = \frac{(\gamma+1)\,A_r\delta}{2\pi d^2_{ij}} \left(\frac{\mathbf{t}^T_j\mathbf{v}_{ji}}{\|\mathbf{v}_{ji}\|}\right)^{\gamma} \frac{-\mathbf{v}^T_{ji}\mathbf{u}_i}{\|\mathbf{v}_{ji}\|}. \tag{4}$$

Consequently, h_{ij} can be expressed as

$$h_{ij} = q_{ij}p_{ij}, \tag{5}$$

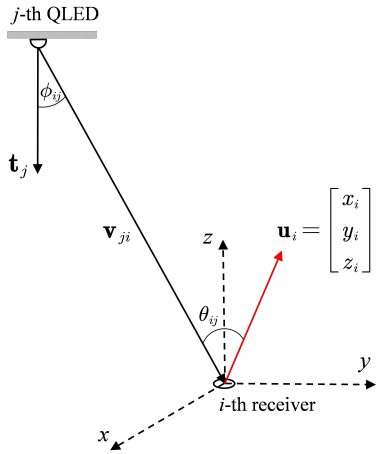

Figure 2. Transmitter and receiver geometry.

where $q_{ij} = \frac{-(\gamma+1)A_r\delta}{2\pi d_{ij}^2\|\mathbf{v}_{ji}\|}\left(\frac{\mathbf{t}_j^T\mathbf{v}_{ji}}{\|\mathbf{v}_{ji}\|}\right)^{\gamma}$ and $p_{ji} = \mathbf{v}_{ji}^T\mathbf{u}_i$. Theoretically, the vector $\mathbf{u}_i$ will directly affect the value of the channel coefficient h_{ij}. Moreover, to better represent the received signal according to the orientation vectors of all receivers, we have

$$\mathbf{r}_m = \mathbf{H}\mathbf{x}_m + \mathbf{n} = \left(\mathbf{x}_m^T \otimes \mathbf{I}_{4N_r}\right) \mathrm{vec}\left(\mathbf{H}\right) + \mathbf{n}. \tag{6}$$

With the results from Equations (2) and (5), we can write $\mathrm{vec}\left(\mathbf{H}\right) = \mathrm{vec}\left(\hat{\mathbf{H}}\right) \circ \mathrm{vec}\left(\mathbf{W}\right) = \mathrm{vec}\left(\mathbf{P}\right) \circ \mathrm{vec}\left(\mathbf{Q}\right) \circ \mathrm{vec}\left(\mathbf{W}\right)$ and so

$$\mathbf{r}_m = \left(\mathbf{x}_m^T \otimes \mathbf{I}_{4N_r}\right) \left[\mathrm{vec}\left(\mathbf{P}\right) \circ \mathrm{vec}\left(\mathbf{Q}\right) \circ \mathrm{vec}\left(\mathbf{W}\right)\right] + \mathbf{n}, \tag{7}$$

where q_{ij} corresponds to the element in the i-th row and j-th column of the $4N_t \times 4N_r$ matrix $\mathbf{Q}$. Similarly, p_{ij} corresponds to the element in the i-th row and the j-th column of the matrix $\mathbf{P}$. Moreover, since $p_{ij} = \mathbf{v}_{ji}^T\mathbf{u}_i$, we can express

$$\mathrm{vec}\left(\mathbf{P}\right) = \mathbf{K}\mathbf{U}, \tag{8}$$

where $\mathbf{U} = \left[\mathbf{u}_1^T, \mathbf{u}_2^T, ..., \mathbf{u}_{N_r}^T\right]^T$. In addition, $\mathbf{K} = \mathbf{1}_{4\times 1} \otimes \mathbf{G}$ where $\mathbf{G} = \begin{bmatrix} \mathbf{G}_1 & \mathbf{0} & \mathbf{0} \\ \mathbf{0} & \ddots & \mathbf{0} \\ \mathbf{0} & \mathbf{0} & \mathbf{G}_{N_r} \end{bmatrix}$ and $\mathbf{G}_i = \mathbf{1}_{4\times 1} \otimes \begin{bmatrix} \mathbf{v}_{i1}^T \\ \vdots \\ \mathbf{v}_{iN_t}^T \end{bmatrix}$. Note that $\mathrm{vec}\left(\mathbf{Q}\right)$, $\mathrm{vec}\left(\mathbf{W}\right)$ are the vectors of size $16N_tN_r \times 1$; $\mathbf{K}$ and $\mathbf{U}$ are of sizes $16N_tN_r \times 12$ and 12×1, respectively. Finally, we have

$$\begin{aligned} \mathbf{r}_m &= \left(\mathbf{x}_m^T \otimes \mathbf{I}_{4N_r}\right) \left[\left(\mathbf{K}\mathbf{U}\right) \circ \mathrm{vec}\left(\mathbf{Q}\right) \circ \mathrm{vec}\left(\mathbf{W}\right)\right] + \mathbf{n} \\ &= \left(\mathbf{x}_m^T \otimes \mathbf{I}_{4N_r}\right) \mathbf{C}\mathbf{U} + \mathbf{n} = \mathbf{B}_m\mathbf{U} + \mathbf{n}, \end{aligned} \tag{9}$$

where $\mathbf{C}$ is a $16N_tN_r \times 12$ matrix with each row $\mathbf{c}_z$ computed by $\mathbf{c}_z = q_z w_z \mathbf{k}_z$ and $\mathbf{B}_m = \left(\mathbf{x}_m^T \otimes \mathbf{I}_{4N_r}\right) \mathbf{C}$. In here, $\mathbf{k}_z$ is the z-th row of matrix $\mathbf{K}$, q_z and w_z are the corresponding z-th elements of $\mathrm{vec}\left(\mathbf{Q}\right)$ and $\mathrm{vec}\left(\mathbf{W}\right)$, respectively.

On the other hand, since the ML detector is utilized, the minimum ED between any two received symbols should be maximized in order to minimize the error probability [3]. Therefore, the orientation

of receivers can be optimized to improve the system performance by solving the following ED-based decision metric optimization

$$\{\mathbf{u}_1, ..., \mathbf{u}_{N_r}\} = \arg \max_{\mathbf{u}_i} \min_{\mathbf{x}_m \neq \mathbf{x}_n \in \mathcal{S}} \|\mathbf{H}(\mathbf{x}_m - \mathbf{x}_n)\|^2, \tag{10}$$

where $\mathbf{u}_i$ denotes the coordinate of the normal vector of the i-th receiver. The normal vector $\mathbf{u}_i$ consequently determines the orientation of the multi-color PDs belonging to the i-th receiver and the receiver design problem becomes the problem of finding the optimal set of $\{\mathbf{u}_1, \mathbf{u}_2, ..., \mathbf{u}_{N_r}\}$. We assumed that the PD cluster belongs to each multi-color receiver as a point; thus, the orientation of the four PDs of the i-th receiver can be adjusted according to the normal vector $\mathbf{u}_i$. Therefore, in theory, to improve the performance of multiple transmitter elements in a VLC system, we can carefully alter the receiver orientation according to (10). The later sections will explain the novel methods used to design the normal vectors such as orientation parameters can be utilized to aid the information transmission for a practical VLC system.

3.2. Proposed Solution

Based on the criterion in (10), the normal vectors optimization problem can be formulated as follows with additional constraints:

$$\text{(P1):} \quad \max_{\mathbf{u}_i, \theta_{ij}} \min_{\mathbf{x}_m \neq \mathbf{x}_n \in \mathcal{S}} \|\mathbf{H}(\mathbf{x}_m - \mathbf{x}_n)\|^2 \tag{11a}$$

$$s.t. \quad 0 < \theta_{ij} \leqslant \theta_{\text{fov}}, \tag{11b}$$

$$\|\mathbf{u}_i\|^2 = 1, \tag{11c}$$

where constraints $\|\mathbf{u}_i\|^2 = 1$ to ensure the normalization assumption for $i = 1, 2, ..., N_r$ and lead to the constraint $(\mathbf{I}_{N_r} \otimes \mathbf{1}_{3\times 1}) \|\mathbf{U}\|^2 = \mathbf{1}_{N_r \times 1}$. Moreover, the condition $0 < \theta_{ij} \leqslant \theta_{\text{fov}}$ aims to ensure that the QLEDs are inside the FOV of the PDs, and can be expressed as $\cos\theta_{\text{fov}} \leqslant \hat{\mathbf{v}}_{ji}^T \mathbf{u}_i < 1$ or $(\cos\theta_{\text{fov}})\mathbf{1}_{N_t N_r \times 1} \leqslant \mathbf{KU} < \mathbf{1}_{N_t N_r \times 1}$. Furthermore, the objective function (11a) can be rewritten as

$$\begin{aligned} \|\mathbf{H}(\mathbf{x}_m - \mathbf{x}_n)\|^2 &= \|(\mathbf{B}_m - \mathbf{B}_n)\mathbf{U}\|^2 \\ &= \mathbf{U}^T (\mathbf{B}_m - \mathbf{B}_n)^T (\mathbf{B}_m - \mathbf{B}_n)\mathbf{U} \\ &= \mathbf{U}^T \mathbf{S}_{mn} \mathbf{U}, \end{aligned} \tag{12}$$

where $\mathbf{S}_{mn} = (\mathbf{B}_m - \mathbf{B}_n)^T (\mathbf{B}_m - \mathbf{B}_n)$.

Consequently, with the additional slack variable α, the optimization problem (P1) can be equivalently transformed into

$$\text{(P2):} \quad \max_{\mathbf{u}_i, ..., \mathbf{u}_{N_r}} \alpha \tag{13a}$$

$$s.t. \quad \mathbf{U}^T \mathbf{S}_{mn} \mathbf{U} \geqslant \alpha, \tag{13b}$$

$$(\cos\theta_{\text{fov}})\mathbf{1}_{N_t N_r \times 1} \leqslant \mathbf{KU} < \mathbf{1}_{N_t N_r \times 1}, \tag{13c}$$

$$(\mathbf{I}_{N_r} \otimes \mathbf{1}_{3\times 1}) \|\mathbf{U}\|^2 = \mathbf{1}_{N_r \times 1}. \tag{13d}$$

The optimization problem (P2) is still nonconvex because of constraints (13b) and (13d); and the global solution for (P2) is an NP-hard problem. Constraint (13d) can be split into two sub-constraints

$$(\mathbf{I}_{N_r} \otimes \mathbf{1}_{3\times 1}) \|\mathbf{U}\|_2^2 \leqslant \mathbf{1}_{N_r \times 1}, \tag{14a}$$

$$(\mathbf{I}_{N_r} \otimes \mathbf{1}_{3\times 1}) \|\mathbf{U}\|_2^2 \geqslant \mathbf{1}_{N_r \times 1}. \tag{14b}$$

To deal with the nonconvex constraints (13b) and constraint (14b), by denoting $\mathbf{U}^{(l)}$ as the value of $\mathbf{U}$ at the l-th iteration and employing the first-order Taylor series expansion around $\mathbf{U}^{(l)}$, the left-hand side of the inequality in (13b) and (14b) can be approximated by

$$\mathbf{U}^T\mathbf{S}_{mn}\mathbf{U} \approx 2\left(\mathbf{U}^{(l)}\right)\mathbf{S}_{mn}\mathbf{U}^T - \left(\mathbf{U}^{(l)}\right)^T\mathbf{S}_{mn}\mathbf{U}^{(l)}, \tag{15}$$

and

$$\begin{aligned}&\left(\mathbf{I}_{N_r}\otimes\mathbf{1}_{3\times1}\right)\|\mathbf{U}\|^2\\ &\quad\approx\left(\mathbf{I}_{N_r}\otimes\mathbf{1}_{3\times1}\right)\left[2\left(\mathbf{U}^{(l)}\right)^T\mathbf{U} - \left(\mathbf{U}^{(l)}\right)^T\mathbf{U}^{(l)}\right].\end{aligned} \tag{16}$$

Finally, by inserting (15) and (16), the optimization problem (P2) can be reformed as

$$\text{(P3):}\quad \max_{\mathbf{U}}\alpha \tag{17a}$$

$$s.t.\quad 2\left(\mathbf{U}^{(l)}\right)\mathbf{S}_{mn}\mathbf{U}^T - \left(\mathbf{U}^{(l)}\right)^T\mathbf{S}_{mn}\mathbf{U}^{(l)} \geqslant \alpha, \tag{17b}$$

$$\left(\cos\theta_{\text{fov}}\right)\mathbf{1}_{N_tN_r\times1} \leqslant \mathbf{KU} < \mathbf{1}_{N_tN_r\times1}, \tag{17c}$$

$$\left(\mathbf{I}_{N_r}\otimes\mathbf{1}_{3\times1}\right)\mathbf{U}^T\mathbf{U} \leqslant \mathbf{1}_{N_r\times1}, \tag{17d}$$

$$\left(\mathbf{I}_{N_r}\otimes\mathbf{1}_{3\times1}\right)\left[2\left(\mathbf{U}^{(l)}\right)^T\mathbf{U} - \left(\mathbf{U}^{(l)}\right)^T\mathbf{U}^{(l)}\right] \geqslant \mathbf{1}_{N_r\times1}. \tag{17e}$$

Clearly, (P3) is a convex optimization problem that can be solved by the CVX package [11,12]. A favorable error performance in the simulations can be achieved with a wise choice of initial solution. Therefore, a number of different initial solutions is necessary. To obtain different initial solutions of $\mathbf{U} = \left[\mathbf{u}_1^T, \mathbf{u}_2^T, \ldots, \mathbf{u}_{N_r}^T\right]^T$, a method is required to generate a number of initial vectors $\mathbf{u}_i$ for the i-th receiver. Since, with each receiver, the set of all normal vectors constructs a sphere with the center the location of the receiver and the radius being equal to one. Therefore, for each multi-color receiver, we divide the unit sphere to $2N$ points with N being the number of initial solution corresponding to the number of initial vector $\mathbf{u}_i$ for each receiver. For $1 \leqslant t \leqslant N$, the normal vectors can be calculated using α_t and β_t, defined as [10]

$$\alpha_t = \arccos\left(v_t\right), \tag{18}$$

and

$$\beta_t \approx \begin{cases} 0, & t = 1, \\ \left(\beta_{t-1} + \frac{2.5456}{\sqrt{N\left(1-v_t^2\right)}}\right) \bmod 2\pi, & 2 \leqslant t \leqslant N, \end{cases} \tag{19}$$

where $v_t = 1 - \frac{2(t-1)}{2N-1}$ and the "mod 2π" notation is to ensure that $\beta_t \in [0, 2\pi]$. Finally, the t-th initial vector for each receiver can be computed by

$$\mathbf{u}_i(t) = \begin{bmatrix} x_i(t) \\ y_i(t) \\ z_i(t) \end{bmatrix} = \begin{bmatrix} \sin\alpha_t\cos\beta_t \\ \sin\alpha_t\sin\beta_t \\ \cos\alpha_t \end{bmatrix}. \tag{20}$$

The design procedure of the proposed technique is summarized in Algorithm 1. Through each iteration, the algorithm exploits the convex problem with the aid of the Taylor approximation method. Moreover, to reduce the computational complexity, two stages are defined. In the first stage, the algorithm solves the optimization problem (P3) with different initial solutions $\mathbf{U}^{(0)}$ but through a small number of iterations. Through our simulation, three iterations are generally enough

for discovering a coarse solution for each initial $\mathbf{U}^{(0)}$. Then, in the second stage, the best coarse solution can be refined until it satisfies the convergence condition ς.

Algorithm 1 Proposed algorithm.

Input: Set of N_{initial} initial vectors $\left\{\mathbf{U}_1, \mathbf{U}_2 ..., \mathbf{U}_{N_{\text{initial}}}\right\}$ that each of $\mathbf{U} = \left[\mathbf{u}_1^T, \mathbf{u}_2^T, ..., \mathbf{u}_{N_r}^T\right]^T$ satisfies $0 < \theta_{ij} \leqslant \theta_{\text{fov}}, \forall i, j$.
Output: Optimal $\mathbf{U}_{\text{opt}}$

First, stage: Coarse solution finding.
for $ite = 1{:}N_{\text{initial}}$ **do**
  set $\mathbf{U}^{(0)} = \mathbf{U}_{ite}; \alpha_{\max} = 0$
  for $l = 0 : 2$ **do**
    normalize $\mathbf{U}^{(l)}$ by setting $\mathbf{u}_i^{(l)} = \frac{\mathbf{u}_i^{(l)}}{\|\mathbf{u}_i^{(l)}\|}$
    solve (P3) with input $\mathbf{U}^{(l)}$ to get $\mathbf{U}_{\text{sol}}$ and $\alpha^{(l)}$
    set $\mathbf{U}^{(l+1)} = \mathbf{U}_{\text{sol}}$
  end for
  if $\alpha^{(l)} > \alpha_{\max}$ **then**
    $\mathbf{U}_{\text{opt}} = \mathbf{U}_{\text{sol}}; \alpha_{\max} = \alpha^{(l)}$
  end if
end for

Second stage: Refine the optimal solution.
set $l = 1; \mathbf{U}^{(0)} = \mathbf{U}_{\text{opt}}; \alpha^{(0)} = \alpha_{\max}$
while $\|\alpha^{(l)} - \alpha^{(l-1)}\| \geqslant \varsigma$ **do**
  normalize $\mathbf{U}^{(l)}$ by setting $\mathbf{u}_i^{(l)} = \frac{\mathbf{u}_i^{(l)}}{\|\mathbf{u}_i^{(l)}\|}$
  solve (P3) with input $\mathbf{U}^{(l)}$ to get $\mathbf{U}_{\text{opt}}$ and $\alpha^{(l)}$
  set $\mathbf{U}^{(l+1)} = \mathbf{U}_{\text{opt}}$
  set $l = l + 1$
end while

3.3. Complexity Analysis

In this section, we provide a discussion on the computational complexity of the proposed algorithm that depends on the optimization-solving process at each iteration and the total number of iterations. During the first stage, only three iterations are necessary for each initial solution while L_{refine} iterations are required in the second stage. Assuming that the interior point method is used by the solver, the order of operations [13] required for solving the convex problem is given by

$$\begin{aligned} &\mathcal{O}\left(M^2 N_{\text{r}}\right) + \left[\mathcal{O}\left(M^3\right) + \mathcal{O}\left(M^2 \begin{pmatrix} M \\ 2 \end{pmatrix}\right)\right] + \mathcal{O}\left(M^2\right) \\ &+ \mathcal{O}\left(N_{\text{r}}\right) = \mathcal{O}\left(M^2 N_{\text{r}}\right) + \mathcal{O}\left(M^4\right), \end{aligned} \tag{21}$$

where $\mathcal{O}\left(M^2 N_{\text{r}}\right)$ denotes the constructing the convex optimization problem, $\mathcal{O}\left(M^3\right) + \mathcal{O}\left(M^2 \begin{pmatrix} M \\ 2 \end{pmatrix}\right)$ denotes the order of operations required during the convex solving process, $\mathcal{O}\left(M^2\right)$ denotes the operations required for computing the first and second derivatives of the objective and constraint functions, and $\mathcal{O}\left(N_{\text{r}}\right)$ denotes the normalization operation, respectively. Consequently, the total complexity cost of the algorithm can be estimated as

$$\begin{aligned} &\mathcal{O}\left(\left(3N_{\text{initial}} + L_{\text{refine}}\right) M^2 N_{\text{r}}\right) + \mathcal{O}\left(\left(3N_{\text{initial}} + L_{\text{refine}}\right) M^4\right) \\ &= \mathcal{O}\left(N_{\text{initial}} M^2 N_{\text{r}}\right) + \mathcal{O}\left(N_{\text{initial}} M^4\right), \end{aligned} \tag{22}$$

where $N_{\text{initial}} \gg L_{\text{refine}}$ in general. It can be seen that the worst case complexity of the algorithm depends on the number of initial solutions, the modulation order, and the number of receivers. In specific scenarios with fixed values of M and N_r, the only variable in (22) is the number of initial solutions N_{initial}. Moreover, as N_{initial} increases, the optimality of the solution in the proposed algorithm also increases. Therefore, N_{initial} is the dominant factor that affects both the complexity and the performance of the system. The trade-off between the computational complexity and the performance improvement through N_{initial} should be carefully considered in order to ensure the specific overall requirement of the receiver.

4. Numerical Results

In this section, we give the results for the proposed and conventional receivers in the VLC system using QLEDs that are presented in a room measuring $4 \times 4 \times 3$ m. We consider a 16×16 MIMO system as there are four RAGB LEDs and four multi-color receivers. The positions of QLEDs are fixed at $(1, 1, 3)$ m, $(1, -1, 3)$ m, $(-1, 1, 3)$ m, $(-1, -1, 3)$ m, respectively. Meanwhile, the receivers are located at two different sets of locations in two scenarios. In Location 1, the receivers are placed near the center as the coordinates are $(0.2, 0.3, 0)$ m, $(0.2, 0.1, 0)$ m, $(0, 0.3, 0)$ m, $(0, 0.1, 0)$ m. In Location 2, the receivers are positioned far from the center with the locations are $(1, 1.1, 1)$ m, $(1, 0.9, 1)$ m, $(0.8, 1.1, 1)$ m, $(0.8, 0.9, 1)$ m.

Moreover, each QLED employs the 4-CSK constellation [7]. Consequently, there are 256 possible symbols for the system of four QLEDs. For simulation with transmission rate of $R = 4, 6$ bps, $M = 16, 64$ symbols are randomly chosen from the set of 256 possible symbols. Moreover, in this paper, we set $\Phi_{1/2} = 60\,\text{deg}, \theta_{\text{fov}} = 60\,\text{deg}, A_r = 1\ \text{cm}^2, \delta = 1\ \text{A/W}$. The signal-to-noise ratio (SNR) is defined as $SNR = \frac{1}{2\sigma^2}$ as transmit power is assumed to be normalized to unity [3]. To find the set of optimal normal vectors for the receivers, the MATLAB optimization toolbox CVX is employed [11]. A set of 200 initial normal vectors $\mathbf{U}$ is utilized to find the optimal orientation for the receivers. On the other hand, as mentioned in previous studies [3,5–10], the conventional receiver generally employs $[0 \quad 0 \quad 1]^T$ as the fixed normal vector since the receiver orientation is usually assumed to be orthogonal to the plane that contains the transmitters.

Figure 3 shows the performance comparison between the proposed, conventional, and the adapted HR [10] for $R = 4$ bps in Location 1 with different crosstalk values. Moreover, the proposed receiver achieves different SNR gains for various ϵ values. When $\epsilon = 0$, the proposed receiver can achieve 3 dB SNR gain while the HR and conventional receiver have almost the same performances. In comparison with the conventional receiver, the proposed receiver can improve the performance by 4 dB in case of $\epsilon = 0.01$ while the gap is only 1 dB in case of $\epsilon = 0.1$. Similarly, in comparison with the HR, the proposed receiver can achieve large SNR gains in the low and medium SNR regimes. The gaps are narrow in the high SNR regimes, but the proposed receiver still maintains better performance in comparison with the HR. Furthermore, the lower the crosstalk level, the better performances of all receivers. Meanwhile, the HR is a low complexity receiver that does not require the orientation adjustment when changing location but can not ensure a favorable and optimal performance in every location.

In Figure 4, we compare the proposed and conventional receivers in both locations when $R = 6$ bps and $\epsilon = 0.01, 0.1$. Since Location 1 is near the center of the room, the correlation between the channel coefficients is high. Therefore, the performance of the conventional receiver in Location 1 is bad. The proposed receiver can significantly alleviate this problem by alternating the normal vectors with the SNR gains that are nearly 4 dB and 2 dB. In addition, in Location 2, the conventional receiver with straight upward normal vectors can not receive sufficient signal power from all QLEDs as in Location 1 and hence the performance becomes worst. However, the proposed receiver with an adequate tuning of the normal vectors can enhance the signal received from all QLEDs. This combines with the inherently low correlation of the MIMO channel in Location 2, dramatically improving the performance. In particular, the receivers in Location 2 have the best performance, and the SNR gains are around 9 dB for both cases of ϵ.

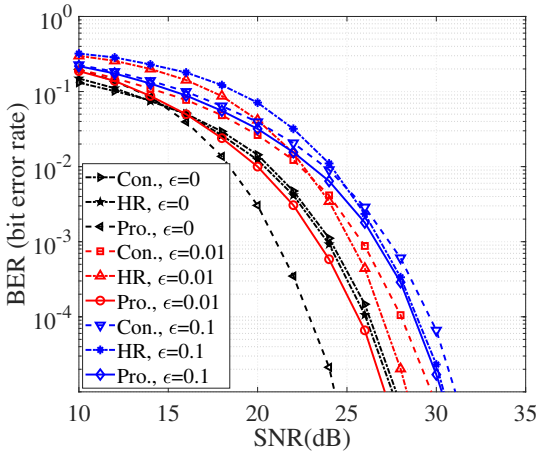

Figure 3. BER performance of the proposed receiver in Location 1 with different crosstalk values when R = 4 bps.

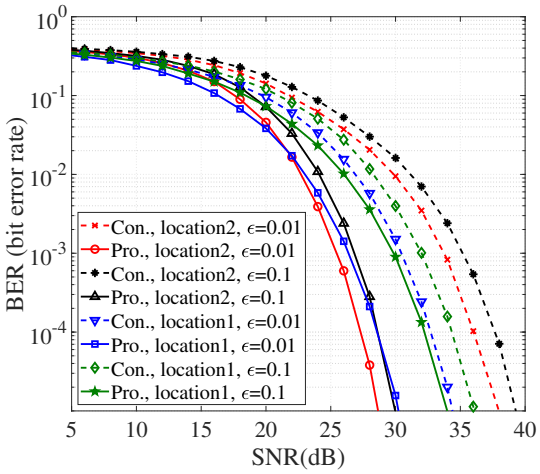

Figure 4. BER performance of the proposed receiver in both locations with different crosstalk values when R = 6 bps.

5. Conclusions

This paper proposes a receiver design for the MIMO-VLC systems composed of QLEDs. The maximization problem of the minimum ED under constraints is obtained by using the normal vector of the receivers. Consequently, the Taylor expansion method is employed to transform the original optimization problem into a convex one that can be solved by an iterative algorithm. Moreover, to reduce the computational complexity, the proposed algorithm, which includes two stages, finds the optimal receiver orientation with different initial solutions. The simulation results show that the proposed receiver provides a better BER performance compared to the various conventional receivers, where the fixed orientation of PD is employed. Moreover, the receiver design algorithms with lower complexity and higher performance, or the consideration of turbulence induced noise [14] in specific scenarios such as underwater and open-path optical communications should be further investigated in the future research.

Author Contributions: Both authors discussed the contents of the manuscript and contributed to its presentation. M.L.T. designed and implemented the proposed scheme, analyzed the simulation results, and wrote the paper under the supervision of S.K.

Funding: This research was funded by the Research Program through the National Research Foundation of Korea (NRF-2019R1A2C1005920).

Conflicts of Interest: The authors declare no conflict of interest.

Abbreviations

The following abbreviations are used in this manuscript:

MIMO	Multiple-input multiple-output
VLC	Visible light communication
LED	Light emitting diode
QLED	Quadrichromatic LED
PD	Photo detector
LOS	Light-of-Sight
NLOS	Non Line of Sight
RAGB	Red/amber/green/blue
ADR	Angle diversity receiver
AWGN	Additive white Gaussian noise

References

1. Komine, T.; Nakagawa, M. Fundamental analysis for visible-light communication system using LED lights. *IEEE Trans. Consum. Electron.* **2004**, *50*, 100–107, [CrossRef]
2. Gong, C. Visible Light Communication and Positioning: Present and Future. *Electronics* **2019**, *8*, 788. [CrossRef]
3. Fath, T.; Haas, H. Performance comparison of MIMO techniques for optical wireless communications in indoor environments. *IEEE Trans. Commun.* **2013**, *61*, 733–742, [CrossRef]
4. Ge, P.; Liang, X.; Wang, J.; Zhao, C.; Gao, X.; Ding, Z. Optical Filter Designs for Multi-Color Visible Light Communication. *IEEE Trans. Commun.* **2018**, *67*, 2173–2187, [CrossRef]
5. Xiao, Y.; Zhu, Y. Chromaticity-adaptive generalized spatial modulation for MIMO VLC with multi-color LEDs. *IEEE Photonics J.* **2019**, [CrossRef]
6. Tang, J.; Zhang, L.; Wu, Z. Exact bit Error rate analysis for color shift keying modulation. *IEEE Commun. Lett.* **2018**, *22*, 284–287, [CrossRef]
7. Liang, X.; Yuan, M.; Wang, J.; Ding, Z.; Jiang, M.; Zhao, C. Constellation design enhancement for color-shift keying modulation of quadrichromatic LEDs in visible light communications. *J. Lightw. Technol.* **2017**, *35*, 3650–3663, [CrossRef]
8. Eroglu, Y.S.; Yapici, Y.; Guvenc, I. Impact of random receiver orientation on visible light communications channel. *IEEE Trans. Commun.* **2018**, *67*, 1313–1325, [CrossRef]
9. Soltani, M.D.; Purwita, A.A.; Tavakkolnia, I.; Haas, H.; Safari, M. Impact of device orientation on error performance of LiFi systems. *IEEE Access* **2019**, *7*, 41690–41701, [CrossRef]
10. Nuwanpriya, A.; Ho, S.W.; Chen, C.S. Indoor MIMO visible light communications: Novel angle diversity receivers for mobile users. *IEEE J. Sel. Areas Commun.* **2015**, *33*, 1780–1792, [CrossRef]
11. Grant, M.; Boyd, S. CVX: Matlab Software for Disciplined Convex Programming. Available online: http://cvxr.com/cvx/ (accessed on 28 June 2019).
12. Tran, M.L.; Kim, S. Layered adaptive collaborative constellation for MIMO visible light communication. *IEEE Access* **2018**, *6*, 74895–74907, [CrossRef]
13. Lee, M.C.; Chung, W.H.; Lee, T.S. Generalized precoder design formulation and iterative algorithm for spatial modulation in MIMO systems with CSIT. *IEEE Trans. Commun.* **2015**, *63*, 1230–1244, [CrossRef]
14. Wu, C.; Ko, J.; Davis, C.C. Imaging through strong turbulence with a light field approach. *Opt. Express* **2016**, *24*, 11975–11986, [CrossRef] [PubMed]